

## Supporting Information

# NIR-Cleavable Drug Adducts of Gold Nanostars for Overcoming Multidrug-Resistant Tumors

*Andrea C. del Valle<sup>a</sup>, Cheng-Kuan Su<sup>b</sup>, Yuh-Chang Sun<sup>a,c</sup>, and Yu-Fen Huang<sup>a,c,\*</sup>*

<sup>a</sup>Department of Biomedical Engineering and Environmental Sciences, National Tsing Hua University, Hsinchu, 30013 Taiwan, ROC

<sup>b</sup>Department of Bioscience and Biotechnology, National Taiwan Ocean University, Keelung, 20224, Taiwan, ROC

<sup>c</sup>Institute of Analytical and Environmental Sciences, National Tsing Hua University, Hsinchu, 30013 Taiwan, ROC

yufen@mx.nthu.edu.tw, Fax: + 886-3-571-8649

## **Supporting Information**

### **Contents**

- 1. Supplementary Material and Methods**
- 2. Supplementary Discussion**
- 3. Supplementary Table**
- 4. Supplementary Figures**

## 1. Supplementary Material and Methods

*Chemicals.* Agarose ultra-grade for molecular biology was obtained from UniRegion Bio-Tech (Taiwan). Bovine serum albumin (BSA), Doxorubicin (DOX), sodium phosphate, EDTA disodium salt, sodium chloride, tetrachloroauric(III) acid, silver nitrate anhydrous (99.9%), sodium dodecyl sulfate (SDS) and Tris were obtained from Sigma-Aldrich (St. Louis, MO, USA). Dulbecco's phosphate-buffered saline (DPBS) was purchased from Biosource (Camarillo, CA, USA). Fetal bovine serum (FBS), penicillin-streptomycin, DMEM, MEM and RPMI-1640 medium were obtained from Gibco (Grand Island, NY, USA). Sybr green I nucleic acid gel stain, 4',6-diamidino-2-phenylindole, dihydrochloride (DAPI), AlexaFluor 633-transferrin and matrigel matrix high concentration were acquired from Invitrogen (Carlsbad, CA, USA). FITC Annexin V/Dead Cell Apoptosis Kit purchased from BD Biosciences (San Jose, CA, USA). The 5'-thiol-modified aptamer, ds(AS1411) (strand 1: 5'-thiol-TTT TTT TTT TTC GAT CGT CGA TCG TCG ATC G-3' and complementary strand 2: 5'-GGT GGT GGT GGT TGT GGT GGT GGT GGT TTT TTC GAT CGA CGA TCG ACG ATC GA-3'), complementary strand 3 for ds(MUC-1): 5'-GCA GTT GAT CCT TTG GAT ACC CTG GT TTT TTC GAT CGA CGA TCG ACG ATC GA-3' and complementary strand 4 for ctrl-dsDNA: 5'-CCT CCT CCT CCT TCT CCT CCT CCT CCT TTT TTC GAT CGA CGA TCG ACG ATC GA-3' were purchased from Genomics BioSci & Tech, Taiwan. HSP70 antibody was purchased from Cell Signaling Technology (Danvers, MA, USA). Alamar blue® was purchased from AbD Serotec (Oxford, UK). Vasculife Basal Medium was purchased from LifeLine Cell Technology (CA, USA). Eosin-Y alcoholic solution, Hematoxylin (MAYERS) solution and Ultra kit (Mounting medium) were obtained from J. T. Baker (Center Valley, PA, USA). TUNEL Assay (Alexa Fluor 647) and SuperFrost Plus Microscope slides were purchased from Thermo Fisher (Massachusetts, USA).

Tissue-Tek OCT cryo gel was purchased from Sakura Finetek (Torrance, CA, USA). Anti-CD31 primary antibody was purchased from Arigo (Taipei, Taiwan). *In vitro* and *in vivo* experiments' reagents, buffers, culture medium and all the aqueous solutions were prepared with deionized water (18.2 M $\Omega$ ·cm), which was sterilized by steam autoclave (121 °C, 40 min) and kept under sterile conditions.

*Synthesis of AuNP.* AuNP were synthesized by citrate reduction, a method previously reported by Frens.<sup>1</sup> Typically, the monodisperse AuNP solution was prepared by boiling 100 mL of 1 mM chloroauric acid. Then, 1.0 mL of 0.4 M trisodium citrate was added; continue heating until color changes from dark blue to red, indicating to the formation of AuNP (12.6  $\pm$  0.8 nm in diameter). The absorption spectrum of AuNP was verified using a UV-3600 spectrophotometer and the resulting concentration was approximately 11 nM according to Beer's law ( $A = \epsilon bc$ ).<sup>2</sup>

*Synthesis of AuNS.* To prepare AuNS, 1 mL of 13 nm seed solution (11 nM) was added to a mixture containing 100 mL of 0.25 mM HAuCl<sub>4</sub> under mild stirring (300 rpm). Then, 1 mL of 2 mM AgNO<sub>3</sub> and 0.5 mL of 100 mM ascorbic acid were simultaneously added to the mixture; the solution was stirred for 30 s (700 rpm) at room temperature. Then, two centrifugation/wash (5000 rcf, 15 min) procedures were performed in order to halt the reaction and AuNS were finally condensed to 1.1 nM in citrate buffer for further experiments.

*Drug Conjugation Efficiency of DOX-dsDNA Complexes.* Samples were subjected to HPLC analyses, which were performed on a C-18 column (ProStar, Varian) with a mobile phase consisting of 10 mM Tris-HCl (pH 7.4) and acetonitrile (5%–50%) in a gradient elution (1% increase per minute) The fraction of Dox remaining bound to the DNA was determined by an

indirect method by calculating the area under the peak corresponding to the unbound Dox at an absorbance of 490 nm relative to a calibration curve.

*Gel Electrophoresis.* Agarose gel for electrophoresis analysis was prepared using 2% agarose in 1× TBE buffer. The solution was heated to 90 °C for 2 min in a microwave and an appropriate amount of Sybr green I was added to the molten solution for DNA visualization. The gel was poured into a horizontal gel tray and allowed to set for 45 min. Samples were diluted (8/10 in volume) in 50% glycerol and loaded onto a gel, followed by running the gel at 90 V in 1× TBE buffer for 15 min. DNA bands were visualized under UV light and each gel image was captured by a 14 megapixel digital camera.

*Cell Line and Buffers.* TRAMP-C1 (transgenic adenocarcinoma of the mouse prostate), MCF 10A (human, mammary gland; breast) and MCF-7 (HTB-22 breast adenocarcinoma) were obtained from American Type Culture Collection (ATCC, Manassas, VA, USA). An adriamycin-resistant cell line MCF-7/ADR was provided by Professor Hsin-Cheng Chiu, National Tsing Hua University, Taiwan. HUVECs (human umbilical vein endothelium cells) were provided by Professor Huan-Tsung Chang, National Taiwan University, Taiwan. Cells were cultured in DMEM medium supplemented with 10% FBS and 1% penicillin-streptomycin, and incubated at 37 °C and 5% CO<sub>2</sub>. HUVECs were growth in Vasculife Basal Medium. Cell density for every experimental assay was determined using a hemocytometer by careful visual microscopic inspection of the nuclei diluted in trypan blue-counting solution.

*In vitro controlled DOX release.* dsDDA-AuNS were dispersed into DPBS of different pH to a final DOX and AuNS concentration of 10.62 μM and 1.1 nM, respectively. Samples were irradiated with a 808 nm CW diode laser (LSR808NL-2000) for 10 min at 0.9 W/cm<sup>2</sup>. After

irradiation, samples were left to cool to room temperature and centrifuged (3500 rcf, 5 min). Subsequently, supernatants were taken for analysis. The pH of the samples was adjusted to 2 with HCl in order to disrupt the electrostatic interaction between DOX and DNA. DOX fluorescence was measured at 600 nm using a microplate reader (Tecan Infinite 200, Tecan Group AG, Basel, Switzerland) with excitation at 480 nm.

*Fluorescence and Dark-Field Microscopy.* Cells were grown onto 10 mm glass coverslip in 48 well plates at a density of  $1 \times 10^5$  cells/well for 12 h. Cells were treated with different conjugates suspended in DMEM medium (10% FBS) for 12 h. For TRAMP-C1 cells, the DOX and AuNS concentrations for 0.1 $\times$  dsDDA-AuNS were 5.8  $\mu$ M (12.5:1 DOX:DNA ratio) and 1.1 nM (0.1 $\times$ ), respectively. For MCF-10A, MCF-7 and MCF-7/ADR cells, the DOX and AuNS concentrations for all samples were kept constant at 11.7  $\mu$ M (12.5:1 DOX:DNA ratio for dsDDA) and 2.2 nM (0.2 $\times$ ). The cells were rinsed twice and fixed with 4% PFA at room temperature for 20 min. Coverslip was mounted onto glass slide using an aqueous mounting medium. Fluorescence and dark-field images were recorded with an inverted fluorescence microscope (Olympus IX71, NY, USA). The scattering light of AuNS conjugates inside cells was recorded with a numerical aperture dark-field condenser (U-DCW, Olympus). Nuclei were visualized after staining with DAPI (1.0  $\mu$ M) for 10 min.

*Drug delivery by dsDDA-AuNS to target cancer cells.* Drug release in cells was evaluated using confocal laser scanning microscopy. All cellular fluorescent images were collected on a Zeiss 780 confocal microscope (Carl Zeiss, Oberkochen, Germany) with a 63 $\times$  oil immersion objective and analyzed using ZEN 2011 software. Cells ( $2 \times 10^5$  in 200  $\mu$ L) were incubated at 37  $^{\circ}$ C with free Dox (10  $\mu$ M) or dsDDA-AuNS (11.7  $\mu$ M Dox equivalents) for 12 h, followed by washing with washing buffer (1 mL) twice at 4  $^{\circ}$ C. Next, cells were then irradiated with NIR laser (1

W/cm<sup>2</sup>, 10 min). Finally, cells were washed twice with washing buffer containing 1% BSA and fixed with 4% paraformaldehyde (PFA) for confocal analysis. Endosome/lysosome marker, AlexaFluor 633-transferrin (70 nM) or LysoTracker (50 μM) was added to the cell solution 30 min prior to analysis of co-localization.

*Apoptosis Assay.* Apoptosis was induced by various stimuli as indicated. Cells were harvested by trypsinization, collected along with the initial culture medium to ensure inclusion of detached cells and pelleted by centrifugation (300 ref, 5 min). Next, Annexin V binding assays were performed using FITC Annexin V Apoptosis Kit. Apoptotic cells were identified by direct visualization of green-colored membrane staining by flow cytometry. To distinguish cells that had lost membrane integrity, propidium iodide (PI) was added to a final concentration of 1 μg/mL before analysis. Staining procedure was performed according to the manufacturer's protocol. Data was analyzed using WinMDI software. Forward and side-scatter profiles were obtained from the same samples.

*HPLC quantification of DOX in tumor tissue homogenates.* Nude mice bearing tumor of about 400 mm<sup>3</sup> was used for intra-tumor DOX quantification. Briefly, mice were treated with DOX (0.125 mg per mouse) and dsDDA-AuNS (0.125 mg of Au and 2.3 μg DOX per mouse) were irradiated with 808 nm laser (0.9 W/cm<sup>2</sup>, 3 min for 3 times) at 24 h and 48 h post intravenous injection. Next, mice were euthanized with CO<sub>2</sub> at 4 h post second laser treatment, and their tumors were harvested. Tissues were subsequently dried, and their weight was measured. Tissue samples were homogenized using a tissue grinder and ultra-sonication process in sterile RIPA Buffer (pH 2). RIPA buffer was added to the samples to obtain final tissue concentration (w/v) of 100 mg/mL. Extraction of DOX was performed twice by adding 3 mL of a chloroform/methanol (9/1, v/v) mixture and stirring for 3 min. Afterwards, samples were centrifuged at 10,000 g per 5

min, the organic phases were collected and further evaporated to dryness at 30 °C. Dry residues were resuspended to a final concentration of 100 mg/mL of mobile phase and 50 µL of the resulting solution was injected into a chromatographic column. Samples were eluted through a Zobrax 300SB C18 (250 mm × 4.6 mm, 5 µm) column (Agilent Technologies). The mobile phase was comprised of 75% Acetonitrile and 25% water in the presence of 0.1% trimethylamine; pH was adjusted to 3 with phosphoric acid. The mobile phase was filtered through a 0.45 µm pore size membrane filter (Millipore, Milford, MA, USA) and sonicated prior use. A constant flow rate of 0.45 mL/min was used for the separation.

## **2. Supplementary Discussion**

### **dsDDA-AuNS show excellent specificity toward nucleolin positive TRAMP-C1 cells.**

As shown in Supplementary Figure S9A a much more intensive signal was observed for dsDDA-AuNS over its non-targeted counterpart against the nucleolin-positive TRAMP-C1 cells. The amount of dsDDA-AuNS taken up by TRAMP-C1 cells was also evaluated via inductively coupled plasma mass spectrometry (ICP-MS). Our result showed that the maximum Au content within cells treated with dsDDA-AuNS followed by repeated washing steps was 20.6 pg/cell, which was almost 5 times higher than that in the ctrl-dsDDA-AuNS group (4.3 pg/cell as shown in Supplementary Figure S9B). The observation of a similar cellular uptake efficiency of dsDNA-AuNS over the non-targeted counterpart (4.5 fold) is indicative of practical retention of recognition capability in aptamer-nanoadducts. Moreover, a relatively weak fluorescence signal was detected in TRAMP-C1 cells using competition analyses competitive binding assays (Supplementary Figure S9C and S10). The high-affinity interaction within dsDDA-AuNS was

unaffected by PEGylation as  $K_d$  was found to be  $0.43 \pm 0.02$  nM (Supplementary Figure S11), which was lower than reported elsewhere.<sup>3</sup> Based on the specific recognition of aptamer-nanoadducts by their target protein, it is considered that the cellular uptake of dsDDA-AuNS by TRAMP-C1 cells took place via a nucleolin-dependent binding and internalization pathway (Supplementary Figure S9D).

**dsDDA-AuNS show selective killing efficiency toward targeted TRAMP-C1 cells through combined photothermal–chemotherapy.**

The selective toxicity of dsDDA-AuNS toward TRAMP-C1 cells was assessed using Alamar Blue assay. As depicted in Supplementary Figure S14A, an increase in the dsDDA-AuNS concentration led to a higher cell death. An additional improvement in cell death was also observed after NIR exposure. Moreover, a gradual decrease in the survival rate of TRAMP-C1 cells was observed depending on the drug to DNA ratios of dsDDA-AuNS (Supplementary Figure S14B). With an increase in laser irradiation power, dsDDA-AuNS also led to higher degrees of cell death compared to dsDNA-AuNS (Supplementary Figure S14C). This result suggests that a pronounced drug activity of dsDDA-AuNS in killing cancer cells was activated by NIR irradiation. As expected, dsDDA-AuNS with a control sequence exerted a negligible toxic effect on TRAMP-C1 cells (data not shown), again confirming that cell-specific recognition is mediated by aptamer AS1411.

Apoptosis induced by chemo-, photo-, or combinational treatment was further evaluated using annexin V and propidium iodide staining (Supplementary Figure S15). The percentage of (dsDDA-AuNS)-treated TRAMP-C1 cells undergoing apoptosis (annexin V+) increased 3.2 fold compared to cells treated with dsDNA-AuNS followed by NIR irradiation (1.7 fold). This

finding is consistent with our previous observation (Supplementary Figure S14A), indicating that NIR-triggered drug release in combined photothermal–chemotherapy can exert greater anti-proliferation activity with respect to living cells. TRAMP-C1 cells treated with dsDNA/DOX-AuNS exhibited more evident increases in apoptosis compared to the aforementioned groups; however, no statistically significant difference in apoptosis ( $p > 0.05$ ) was observed after laser treatment. These results are also supported by observing the degree of intracellular uptake and payload release of drug formulated in different nanoconjugates (Supplementary Figure S16). The nonspecific leakage is indicative of DOX physically associated with dsDNA-AuNS, resulting in high dark toxicity and ineffective NIR controllability of on-demand drug release and DOX-related toxicity. However, a weak DOX signal was initially detected in cells receiving dsDDA-AuNS. A remarkable recovery of the fluorescence signal monitored in cells subjected to additional NIR irradiation was observed, indicating that the photothermal effect on dsDDA-AuNS could accelerate the payload release and inhibit subsequent tumor cell growth by synergistic photothermal and chemotherapy. As shown in Supplementary Figure S17, the degree of HSP70 expression in treated cells is correlated with therapeutic effects against TRAMP-C1 (Supplementary Figure S14A), suggesting that the successful activation of an HSP-dependent apoptotic pathway was achievable by NIR exposure of (dsDDA-AuNS)-treated tumor cells.

### 3. Supplementary Tables

**Table S1**

**Table S1. Drug conjugation efficiency of different DOX-dsDNA complexes.**

Sample	Ratio (DOX:dsDNA)	Bound DOX per dsDNA	Conjugation Efficiency (%)
dsDDA <sub>AS1411</sub>	25:1	9.3	37.2 ± 4.9
dsDDA <sub>AS1411</sub>	12.5:1	6.9	55.1 ± 8.0
dsDNA/DOX <sub>AS1411</sub>	25:1	2.9	11.6 ± 10.6
dsDNA/DOX <sub>AS1411</sub>	12.5:1	0.1	1.2 ± 8.3
ctrl-dsDDA	12.5:1	7.8	56.4 ± 6.7
dsDDA <sub>MUC1*</sub>	12.5:1	9.9	79.5 ± 9.1

\*Adduct reaction with 200 mM KCl and 4 mM MgCl<sub>2</sub>

**Table S2**

**Table S2. Structural features of different nanocomplexes.**

Sample	Zeta Potential (mV)	Size (d. nm)	PdI	No. dsDNA per AuNS	dsDNA Encapsulation Efficiency (%)	DOX Encapsulation Efficiency (%)
AuNS	-35.1 ± 5.1 (citrate)	76.9 ± 6.2	0.54 ± 0.0	-	-	-
Non-PEGlyated dsDNA-AuNS	-32.7 ± 6.4 (DPBS)	90.5 ± 9.9	0.43 ± 0.1	778 ± 18	85.5 ± 2.1	-
dsDNA-AuNS	-13.7 ± 3.2 (DPBS)	93.9 ± 3.0	0.45 ± 0.1	689 ± 102	75.8 ± 11.7	-
dsDDA-AuNS	-8.0 ± 2.1 (DPBS)	96.4 ± 3.9	0.38 ± 0.1	763 ± 50	83.9 ± 5.5	90.4 ± 4.8
dsDNA/DOX-AuNS	-13.7 ± 5.8 (DPBS)	97.8 ± 7.0	0.39 ± 0.2	693 ± 77	76.2 ± 8.4	36.5 ± 6.7

\*The DOX encapsulation efficiency (%) was determined at a feeding ratio of 6.5:1 between DOX and dsDNA.

#### 4. Supplementary Figures

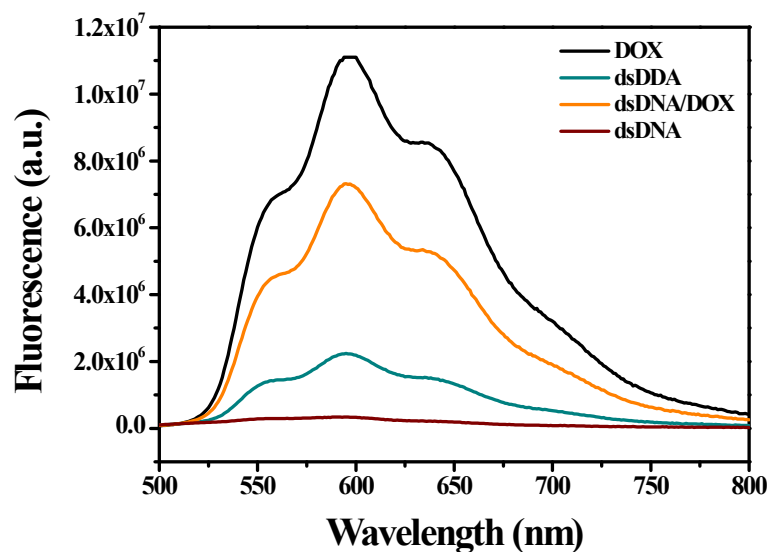
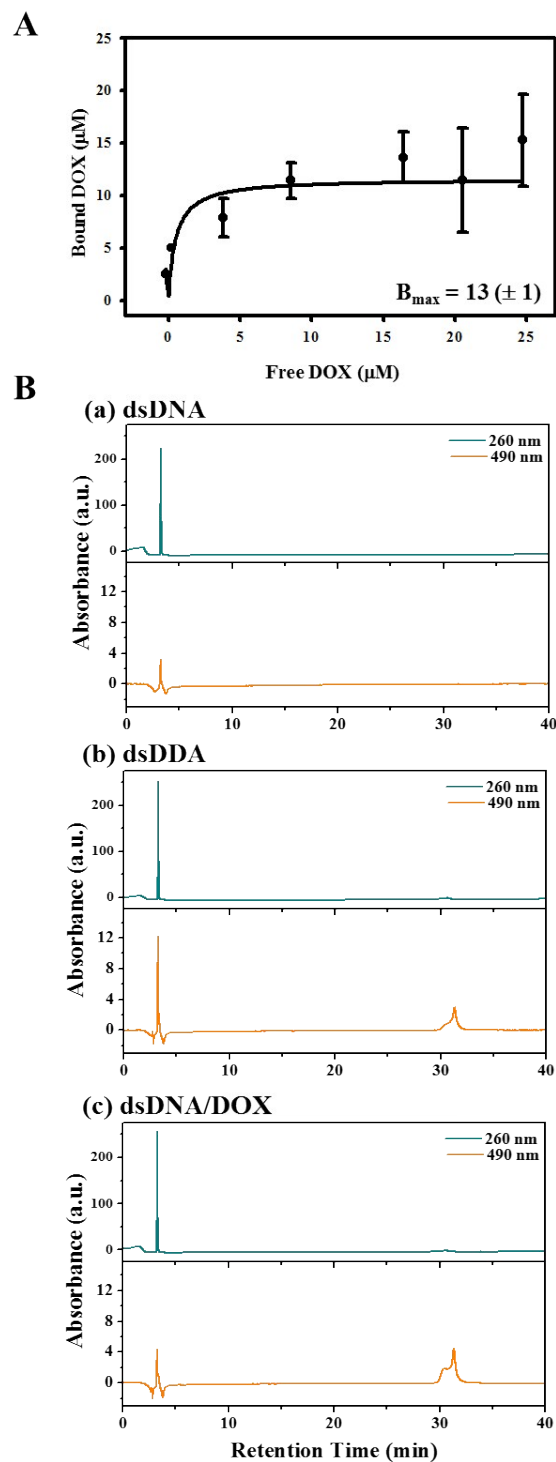
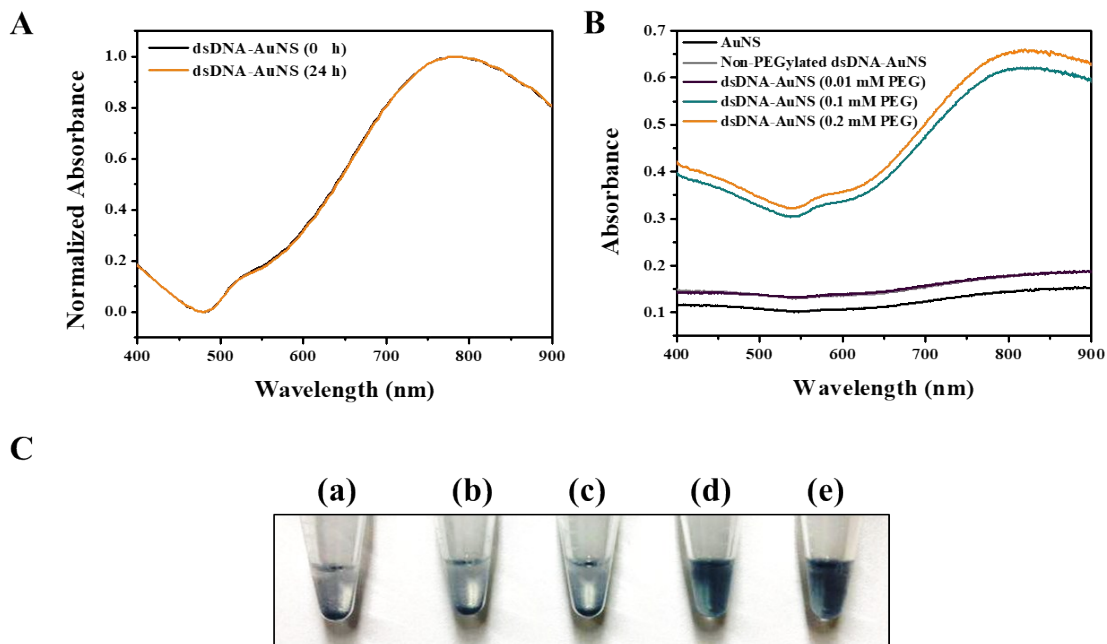


**Figure S1.** Fluorescence spectra of free DOX, dsDDA, dsDNA/DOX (reaction solution without formaldehyde), and dsDNA in phenol red free DMEM medium with 10% FBS. The quenching ratio ( $F/F_0$ ) was higher for covalent dsDDA adduct (80.2%) than that of non-covalent dsDNA/DOX adduct (34.7%; DOX:dsDNA ratio, 12.5:1).

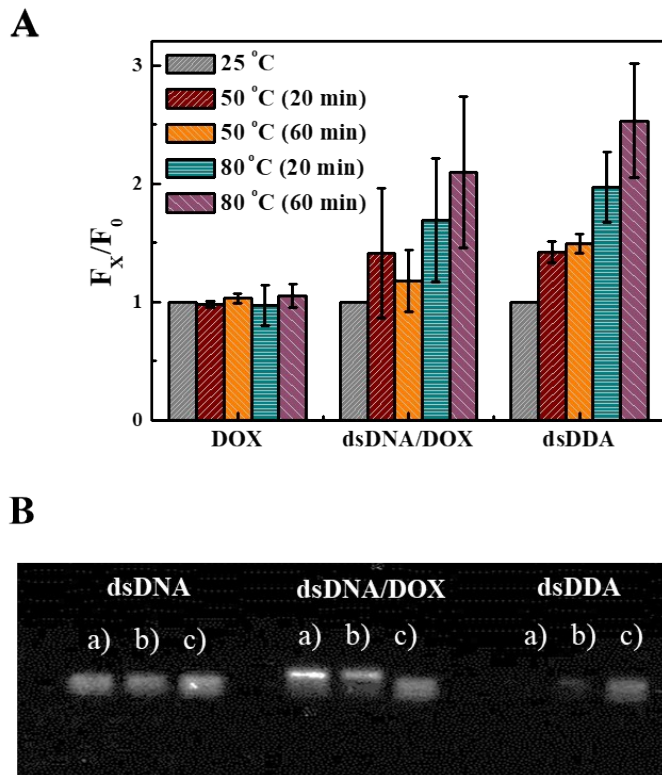


**Figures S2.** DOX loading efficiency of different drug-dsDNA complexes. (A) Analysis of DOX loading to dsDDA adducts. The saturation curve was obtained by exposing ds(AS1411) ( $1.6 \mu\text{M}$ ) to  $2.5\text{--}40 \mu\text{M}$  DOX. (B) HPLC purification data showing the absorbance as a function of

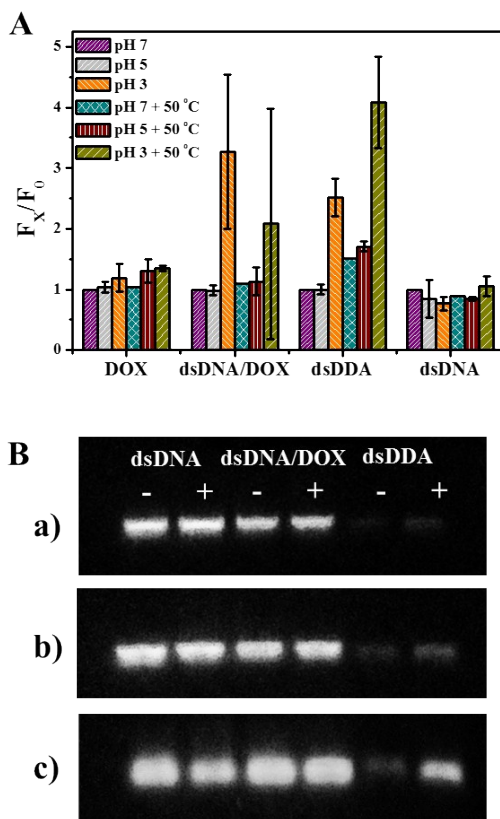
retention time for (a) pure dsDNA, (b) dsDDA, and (c) dsDNA + Dox. The suspension was cleared of unbound DOX by HPLC in a gradient purification using 10 mM Tris-HCl (pH 7.4) and acetonitrile as eluent (5%–50%) with an increase of 1% per minute. Experiments were repeated at least three times.



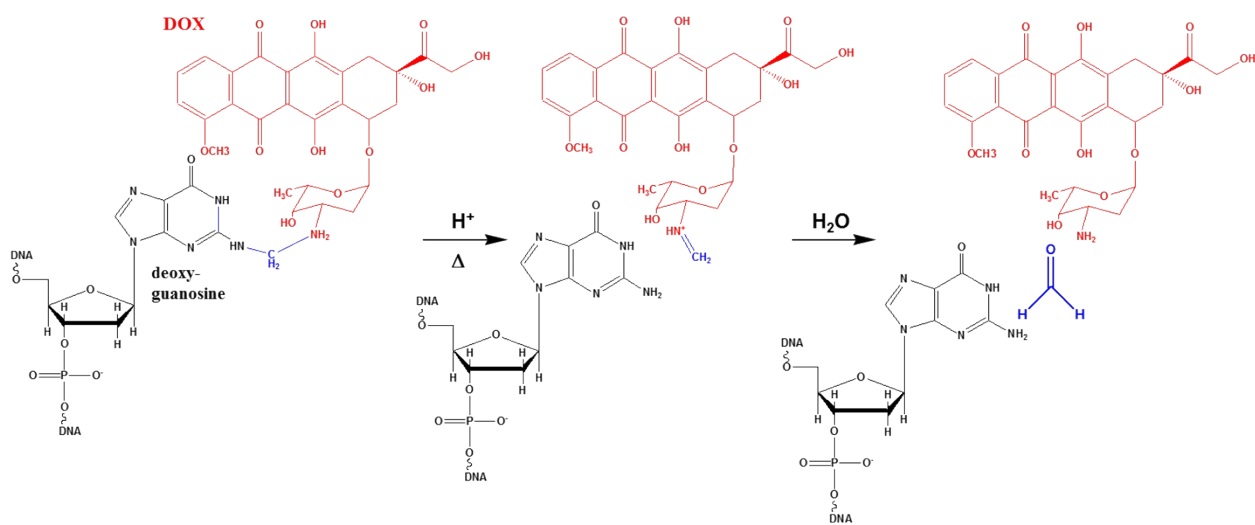
**Figure S3.** (A) UV-Vis absorption of dsDNA-AuNS (0.1 mM PEG) at 0 and 24 h, showing no significant changes in the absorption spectra. (B) UV-Vis absorption and (C) photographs of different samples: (a) AuNS, (b) Non-PEGylated dsDNA-AuNS, (c) dsDNA-AuNS (0.01 mM PEG), (d) dsDNA-AuNS (0.1 mM PEG), and (e) dsDNA-AuNS (0.2 mM PEG) suspended in DPBS for 24 h, showing that the optimal concentration for AuNS PEGylation is 0.1 mM.



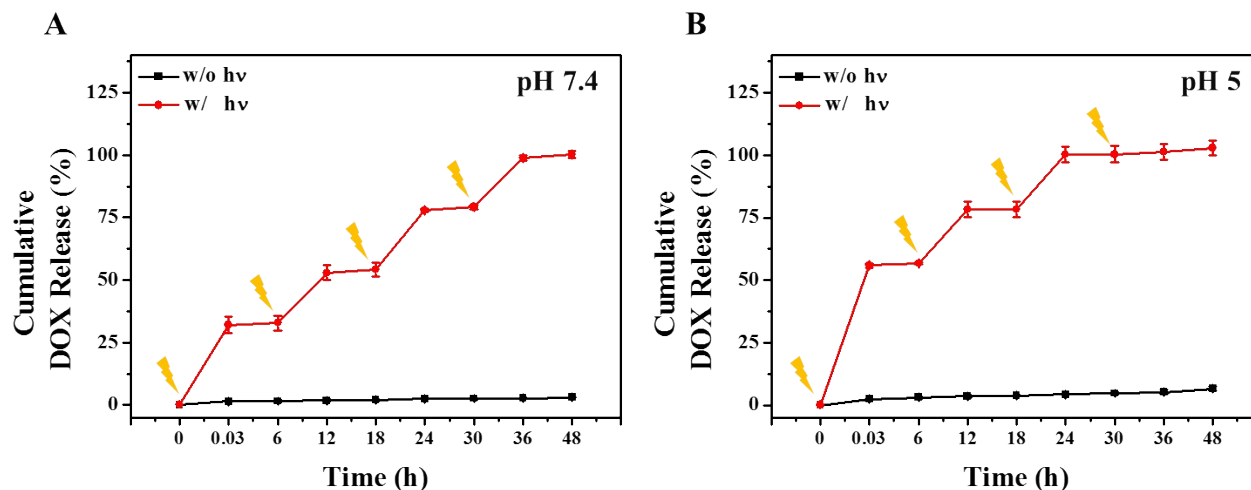
**Figure S4.** (A) Fluorescence recovery of DOX from different drug-DNA complexes and its corresponding  $F_x/F_0$  ratio;  $F_x$  is the fluorescence at a defined incubation condition and  $F_0$  represents the fluorescence signal obtained at 25°C. An increase in the fluorescence intensity indicates a heat labile DOX release from dsDNA/DOX and dsDDA, respectively. (B) 2% agarose gel electrophoresis of dsDNA, dsDNA/DOX, and dsDDA incubated for 60 min at (a) 25°C, (b) 50°C, and (c) 80°C. The fluorescence recovery of dsDDA with Sybr green I staining indicates the detachment of DOX from the drug-DNA moiety. dsDDA presents high stability at room temperature and conditional drug release at 50°C and 80°C, respectively. Experiments were repeated at least three times.



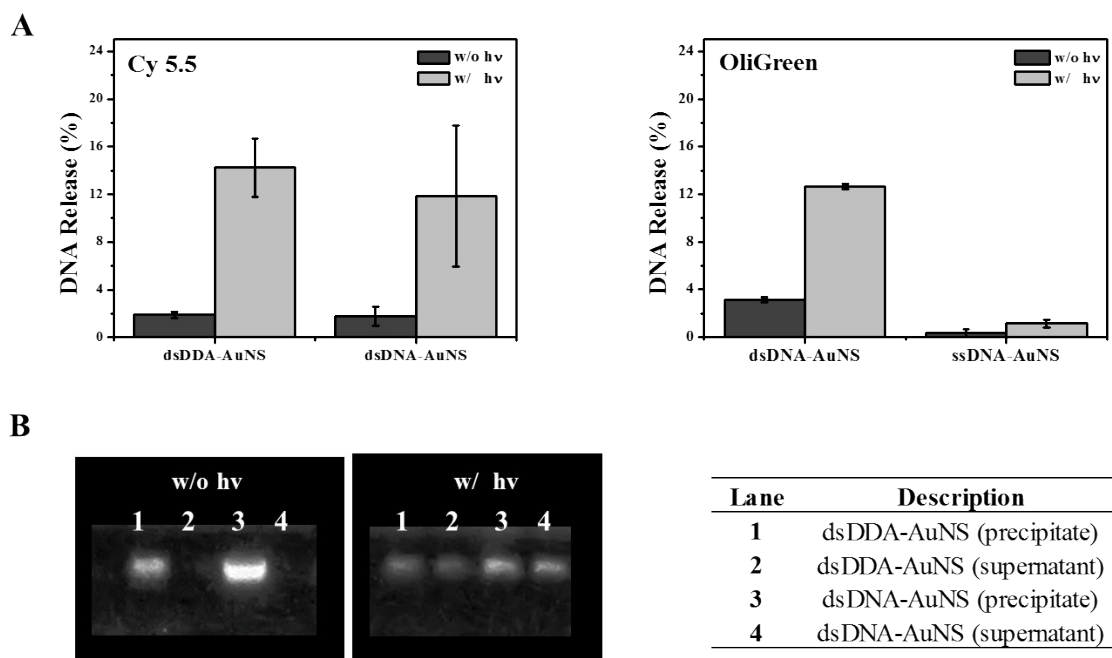
**Figure S5.** (A) Fluorescence recovery of DOX from different drug-DNA complexes and its corresponding  $F_x/F_0$  ratio;  $F_x$  is the fluorescence at a defined incubation condition and  $F_0$  represents the fluorescence signal obtained at 25°C, pH 7. An increase in the fluorescence intensity indicates a heat and acid labile DOX release from dsDNA/DOX and dsDDA, respectively. (B) Agarose gel electrophoresis of dsDNA, dsDNA/DOX, and dsDDA incubated at (a) pH 7, (b) pH 5, and (c) pH 3. Control samples were kept at room temperature 25°C (-), whereas others were heated to 50°C (+) over 20 min. This showed fluorescence recovery of dsDDA with Sybr green I staining. dsDDA presents high stability at pH 7 and room temperature and conditional drug release at low pH and 50°C over 20 min. Experiments were repeated at least three times.



**Scheme S1.** A reversible reaction between DOX and the exocyclic amino group of guanine in DNA is proposed under acidic condition. The cleavable methylene linkage between drug moieties and DNA allows stimuli-responsive controlled drug release.

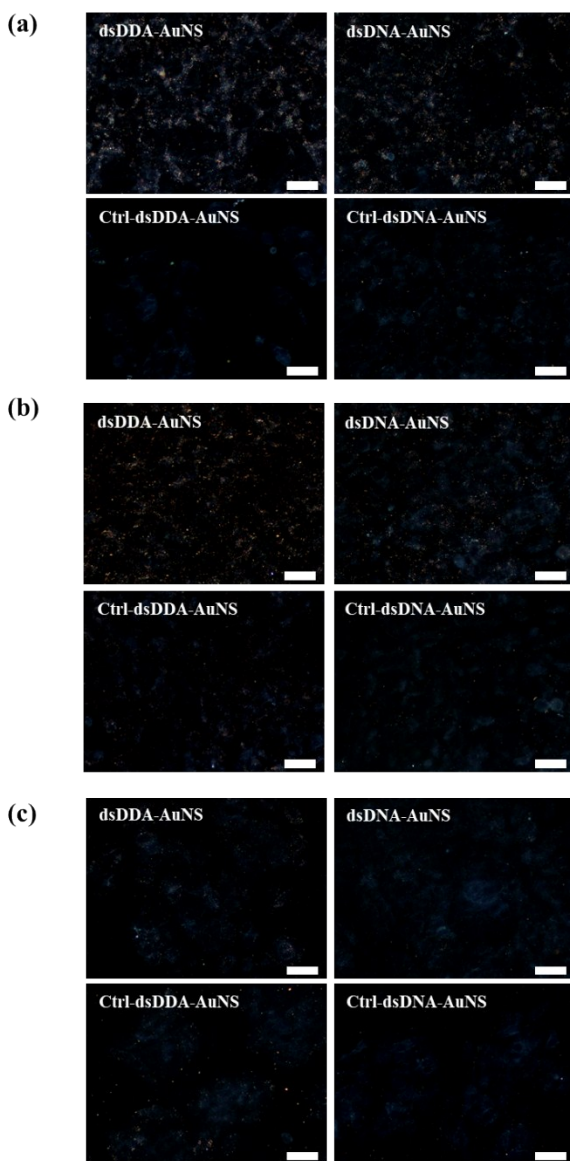
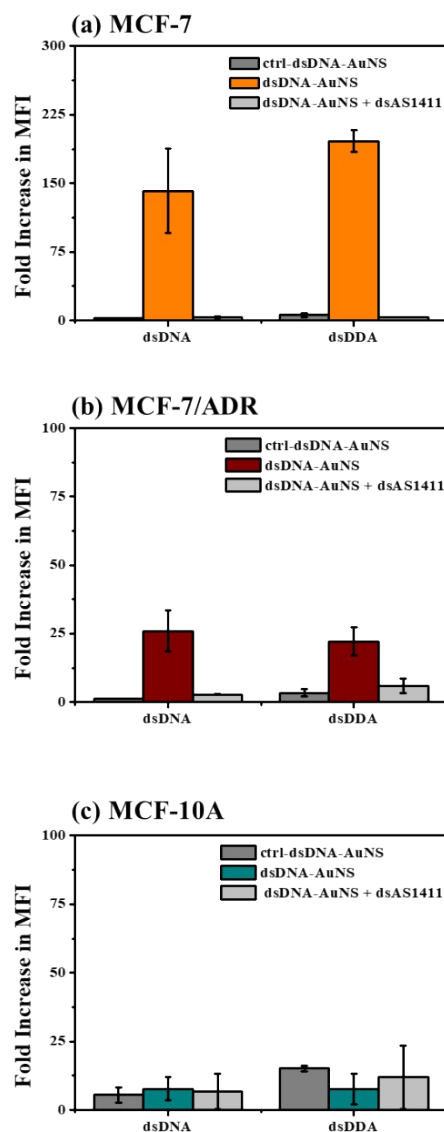


**Figure S6.** Drug release profiles of dsDDA-AuNS in serum condition under NIR irradiation (808 nm, 0.9 W/cm<sup>2</sup>, 2 min). dsDDA-AuNS was incubated in phenol red free DMEM with 10% FBS at 37 °C and at (A) pH 7.4 and (B) pH 5, respectively. The samples were centrifuged (8000 rpm, 10 min); the fresh serum medium was added to the residual mixture and DOX in the supernatants was subjected to fluorescence quantification. Yellow marks indicate the irradiation points.



**Figure S7.** (A) Release percentage of Cy5.5 labeled AS1411 (left) and OliGreen stained ssDNA (right) from different AuNS conjugates before and after laser irradiation (808 nm, 0.9 W/cm<sup>2</sup>, 10 min) at pH 5. For the preparation of dsDDA-AuNS (or dsDNA-AuNS), Cy5.5 labeled or non-labeled AS1411 was hybridized in a 1:1 ratio with the complementary sequence 5' thiol-T<sub>10</sub>(TCGATCG)<sub>3</sub>, followed by AuNS conjugation as described in Experimental details. Oligonucleotides (ssDNA) with sequence of 5' Thiol-T<sub>10</sub> GGT GGT GGT GGT TGT GGT GGT GGT GG-3' was used for the synthesis of ssDNA-AuNS. No loss of total volume was observed while performing the irradiation experiments. Samples were then centrifuged at 3,000 rcf for 5 min to collect the supernatants. Release of Cy5.5 labeled AS1411 was quantified by using a standard curve in the same buffer as the samples. Release of ssDNA was quantified using OliGreen stain. No significant ssDNA release was observed for ssDNA-AuNS. Experiments were repeated at least three times. (B) 1% agarose gel electrophoresis of dsDNA-AuNS and dsDDA-AuNS (2:1 DOX:dsDNA ratio) using Sybr green I staining. No significant DNA leakage

was observed before laser irradiation; however, DNA bands are visible in the supernatants of laser irradiated samples. For all current experiments, samples were initially suspended in DPBS and irradiated with an 808 nm laser for 10 min. No loss of total volume was observed while performing the experiments. Samples were then centrifuged at 3,000 rcf for 5 min to collect the supernatants. Precipitants were suspended in the same buffer as the supernatants and dissolved with NaCN previously loaded in the agarose gel.

**A****B**

**Figure S8.** (A) Representative dark-field microscopy images of (a) MCF-7, (b) MCF-7/ADR, and (c) MCF-10A cells receiving different treatments. Cells were incubated with different conjugates suspended in culture medium (10% FBS) for 12 h; cells were washed twice with washing buffer containing 1% BSA and fixed with 4% PFA. Cover Slides were mounted in ProLong Gold reagent and analyzed by dark-field microscopy. Scale bar: 50 μm. (B) Flow

cytometric competitive binding assay between Cy5.5 labeled dsDNA-AuNS and Cy5.5 labeled dsDDA-AuNS co-incubated with a fixed concentration of dsAS1411 (1  $\mu$ M) for interaction with (a) MCF-7, (b) MCF-7/ADR, and (c) MCF-10A cells. The y-axis represents the fold increase in mean fluorescence intensity compared to unstained control cells. Each experiment was repeated three times. The DOX and AuNS concentrations for all samples were kept constant at 11.7  $\mu$ M (12.5:1 DOX:DNA ratio for dsDDA) and 2.2 nM (0.2 $\times$ ), respectively.

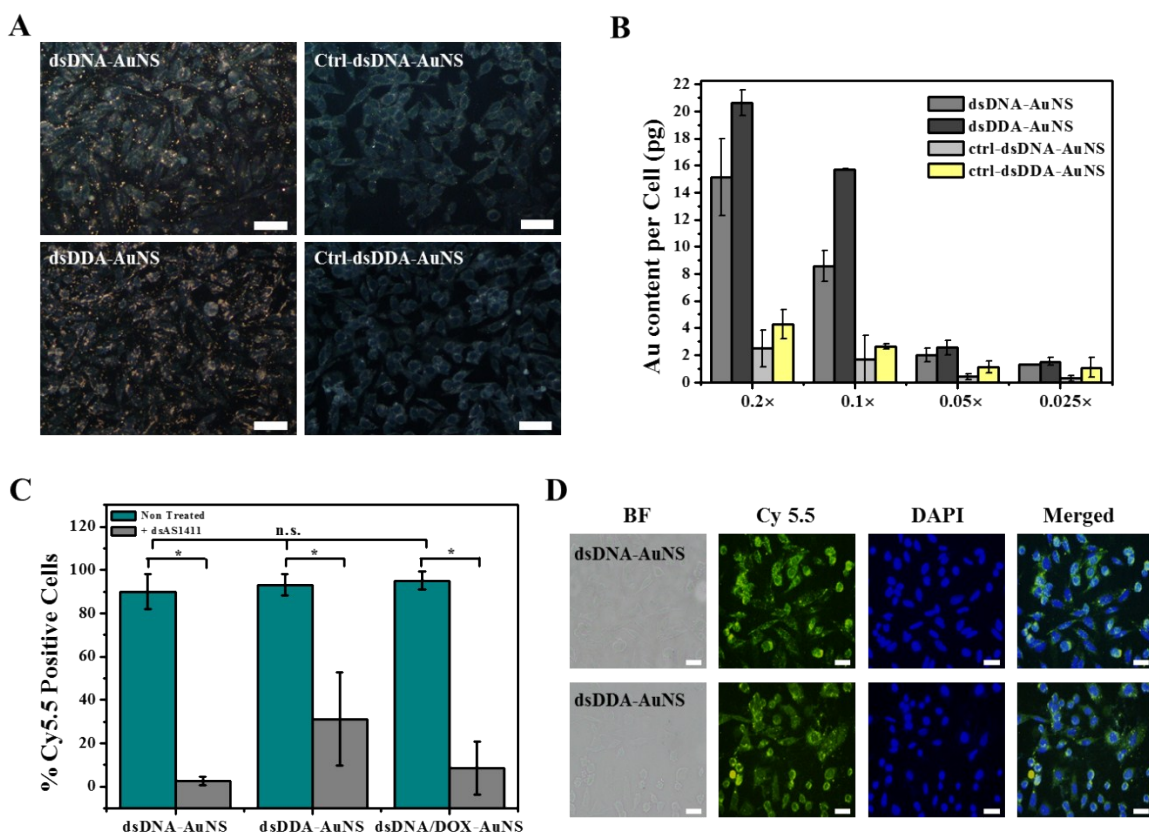


**Figure S9.** (A) Dark-field microscopic images of TRAMP-C1 cells incubated for 12 h with dsDNA-AuNS and dsDDA-AuNS compared with their respective control DNA. (B) Cellular uptake of different nanoconjugates as a function of concentration of dsDNA-AuNS, dsDDA-AuNS, ctrl-dsDNA-AuNS, and ctrl-dsDDA-AuNS. The uptake amount of Au per cell were determined with ICP-MS. (C) Flow cytometric competitive binding assay of dsDDA-AuNS co-incubated with a fixed concentration of dsAS1411 (1  $\mu$ M) for interaction with TRAMP-C1 cells. Cells were incubated with samples for 12 h prior to flow cytometry analysis. The fluorescence intensity of Cy5.5 labeled dsDNA-AuNS, Cy5.5 labeled dsDDA-AuNS, and Cy5.5 labeled dsDNA/DOX-AuNS conjugates was acquired via an APC channel. (n = 3, \*p < 0.05) (D) Microscopy images of TRAMP-C1 cells after 12 h incubation with Cy5.5 labeled dsDNA-AuNS and Cy5.5 labeled dsDDA-AuNS, respectively. Scale Bar: 50  $\mu$ m.

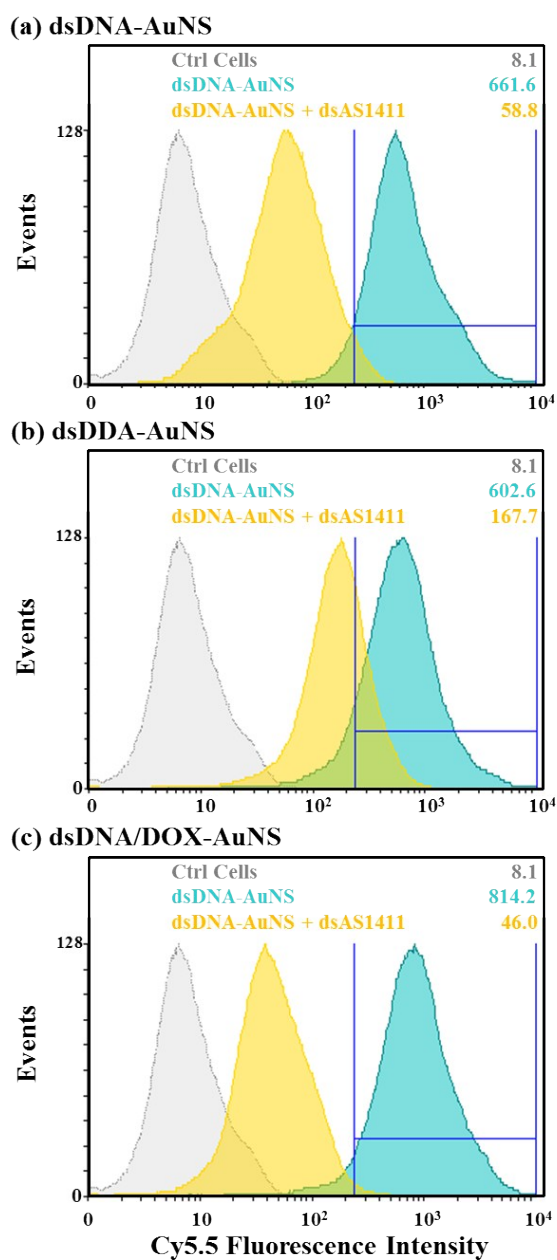


**Figure S10.** Representative flow cytometry histograms for competitive binding assay of (a) dsDNA-AuNS, (b) dsDDA-AuNS, and (c) dsDNA/DOX-AuNS, respectively. Histograms display the fluorescence signal pattern of non-treated TRAMP-C1 cells (gray) and cells receiving different treatments (blue) and co-incubated with excess dsAS1411 (yellow), respectively.

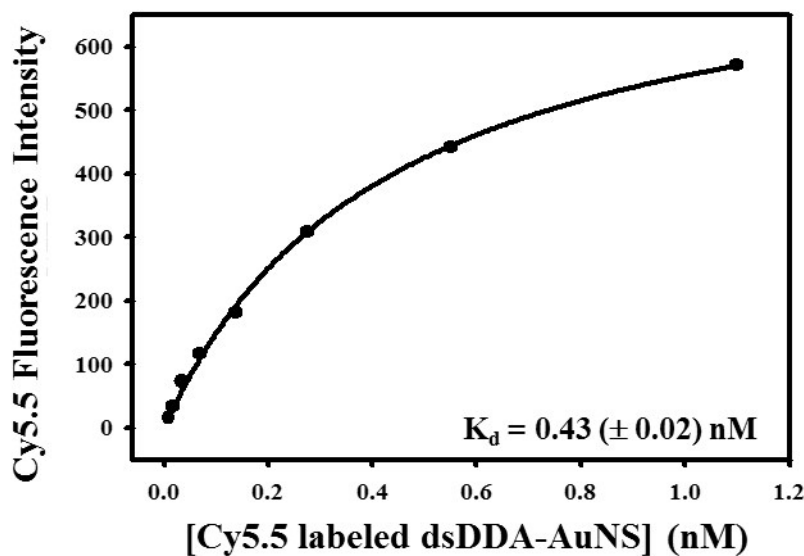


**Figure S11.** Flow cytometry to determine the binding affinity of Cy5.5 labeled dsDDA-AuNS to TRAMP-C1 cells ( $2 \times 10^5$ ). Conjugates were added and incubated in binding buffer (washing buffer containing 1% BSA) on ice for 30 min, followed by washing twice with washing buffer. Precipitated cells were suspended in binding buffer prior to analysis on a BD Biosciences FACScalibur FACScan flow cytometer. Data were analyzed with the WinMDI software. Cy5.5 labeled ctrl-dsDDA-AuNS was used as a negative control to subtract nonspecific interaction. The experiment was repeated five times. The equilibrium dissociation constant ( $K_d$ ) was obtained by fitting the dependence of fluorescence intensity of specific binding on the concentration of fluorescent labeled dsDDA-AuNS to the equation  $Y = B_{\max} \cdot X / (K_d + X)$ , using SigmaPlot (Version 12.5; Systat, San Jose, CA, USA).

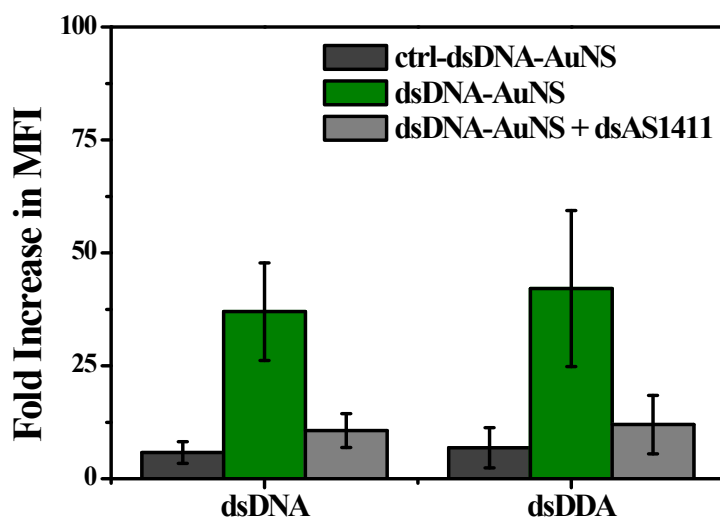


**Figure S12.** Flow cytometric competitive binding assay between Cy5.5 labeled dsDNA-AuNS and Cy5.5 labeled dsDDA-AuNS co-incubated with a fixed concentration of dsAS1411 (1  $\mu$ M) for interaction with HUVECs. The y-axis represents the fold increase in mean fluorescence intensity compared to unstained control cells.

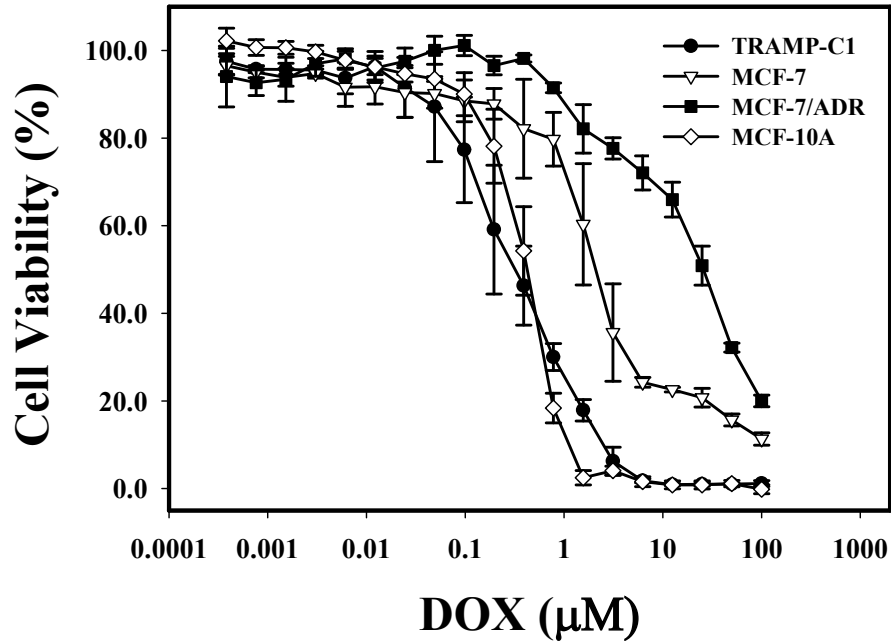


**Figure S13.** Sigmoidal dose-response of different cell lines toward a serial concentration of DOX. The half-maximal inhibitory concentrations ( $IC_{50}$ ) of DOX are  $0.69 \pm 0.07$ ,  $1.57 \pm 0.13$ ,  $12.74 \pm 0.16$ , and  $0.77 \pm 0.08$   $\mu\text{M}$  for TRAMP-C1, MCF-7, MCF-7/ADR, and MCF-10A, respectively. Different cell lines were incubated independently with the drug for 12 h. Afterwards, cells were washed twice with washing buffer and fresh medium was added. Cells were left to recover for 48 h prior to Alamar Blue assay. The equation for sigmoidal fitting was stated as follows:  $Y = \min + (\max - \min) / (1 + 10^{(\log IC_{50} - X)})$  using SigmaPlot. The experiments were performed three to four times.

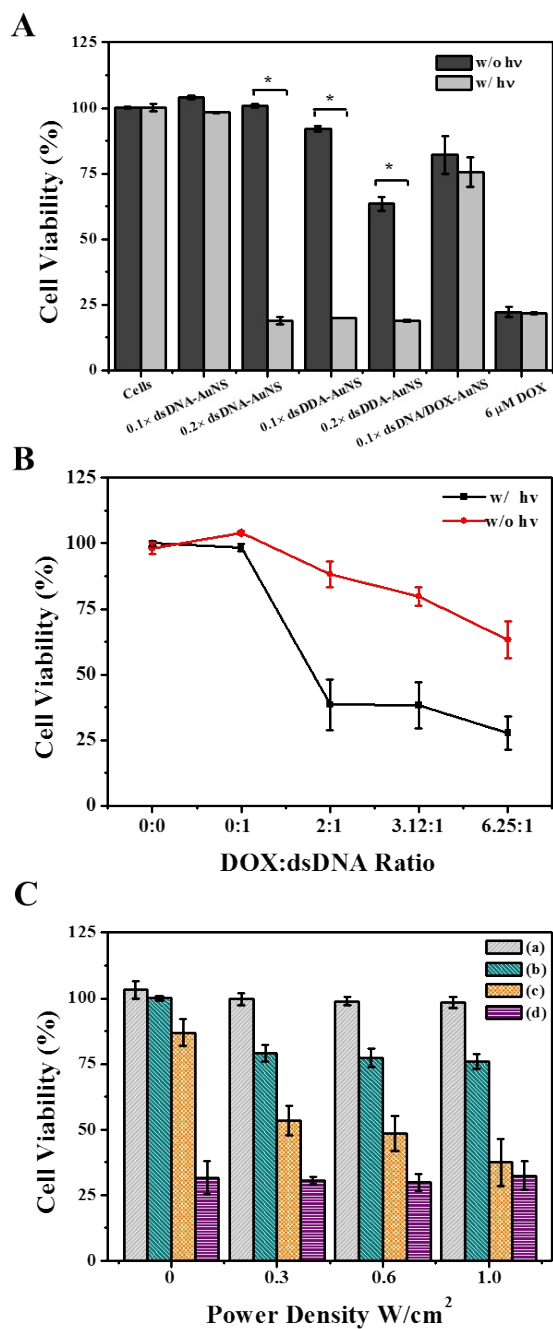


**Figure S14.** Drug-DNA nanoadducts for targeted combination therapy *in vitro*. (A) Cytotoxicity assays of TRAMP-C1 cells under different treatments. The DOX and AuNS concentrations for 0.1× dsDDA-AuNS were 5.8 μM (12.5:1 DOX:DNA ratio) and 1.1 nM, respectively. (B) Dose-response curves of 0.1×dsDDA-AuNS with different DOX:dsAS1411 ratios against targeted

TRAMP-C1 cells. (C) Power-dependent toxicity of (a) non-treated cells and (b) dsDNA-AuNS, (c) dsDDA-AuNS, and (d) free DOX toward TRAMP-C1 cells. The DOX and AuNS concentrations of dsDDA-AuNS were kept constant at 1.6  $\mu$ M (2:1 DOX:DNA ratio) and 1.1 nM (0.1 $\times$ ), respectively. Conjugate incubation was performed in culture medium (10% FBS) at 37°C for 12 h. After drug treatment, cells were exposed to 808 nm irradiation at different power densities for 10 min. Cells were subsequently grown in fresh medium for 48 h. The cytotoxicity was measured by MTT assay. Experiments were repeated at least three times. (n = 3, \*p < 0.05).

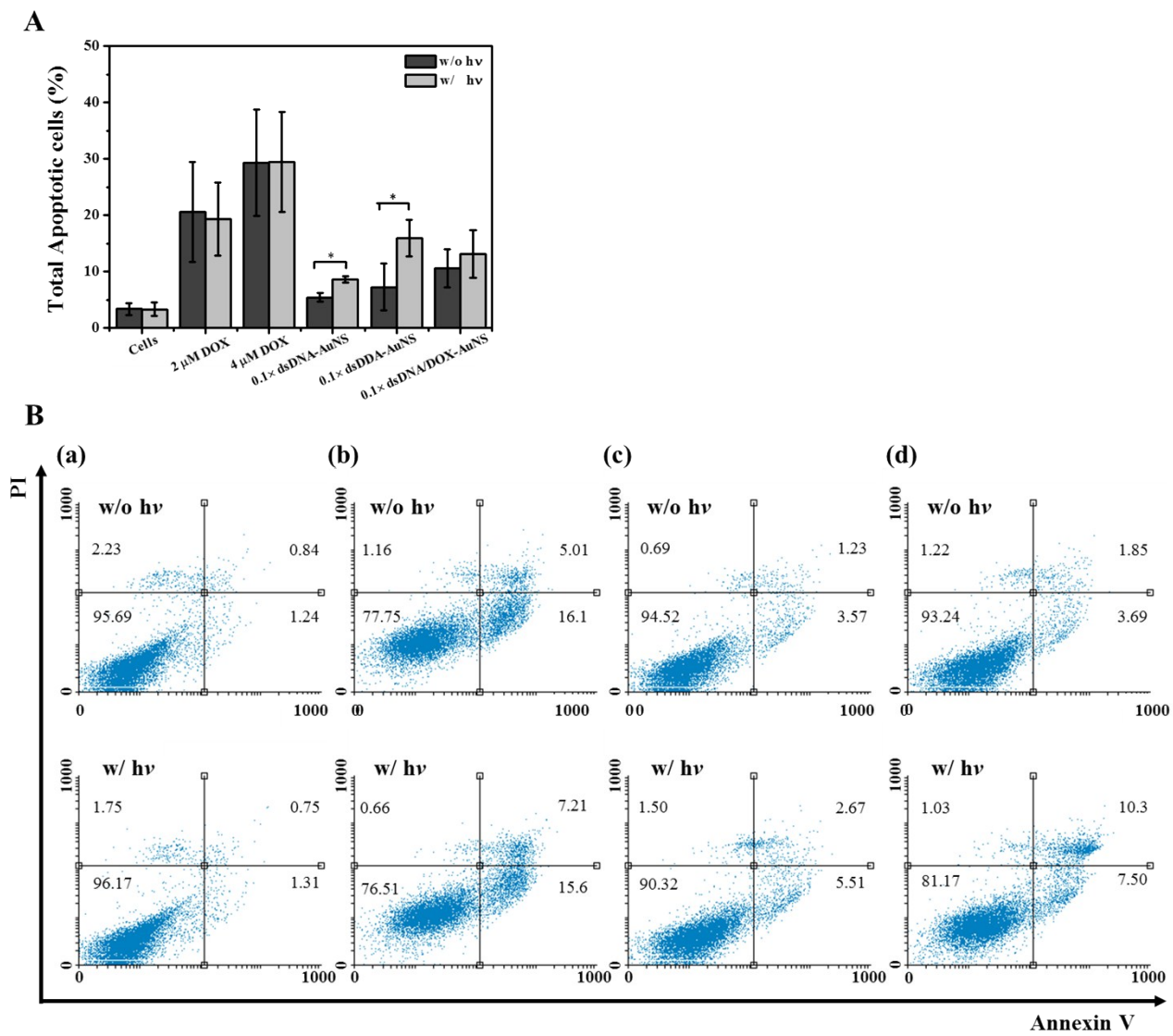


**Figure S15.** Flow cytometry results of TRAMP-C1 cells incubated with different drug conjugates, followed by NIR irradiation. (A) Percentages of apoptotic cells and (B) representative density plots showing the treated cells double stained with annexin V FITC-A vs propidium Iodide-A. TRAMP-C1 cells (a) and cells were incubated with (b) free DOX (4  $\mu$ M), (c) dsDNA-AuNS, and (d) dsDDA-AuNS in culture medium (10% FBS) at 37°C for 12 h. The DOX and AuNS concentrations of dsDDA-AuNS were kept constant at 5.8  $\mu$ M (12.5:1 DOX:DNA ratio) and 1.1 nM (0.1 $\times$ ), respectively. After treatment, cells were exposed to 808 nm

irradiation (1 W/cm<sup>2</sup>) for 10 min. Cells were subsequently grown in fresh medium for 3 h before flow cytometry analysis (n = 3, \*p < 0.05).

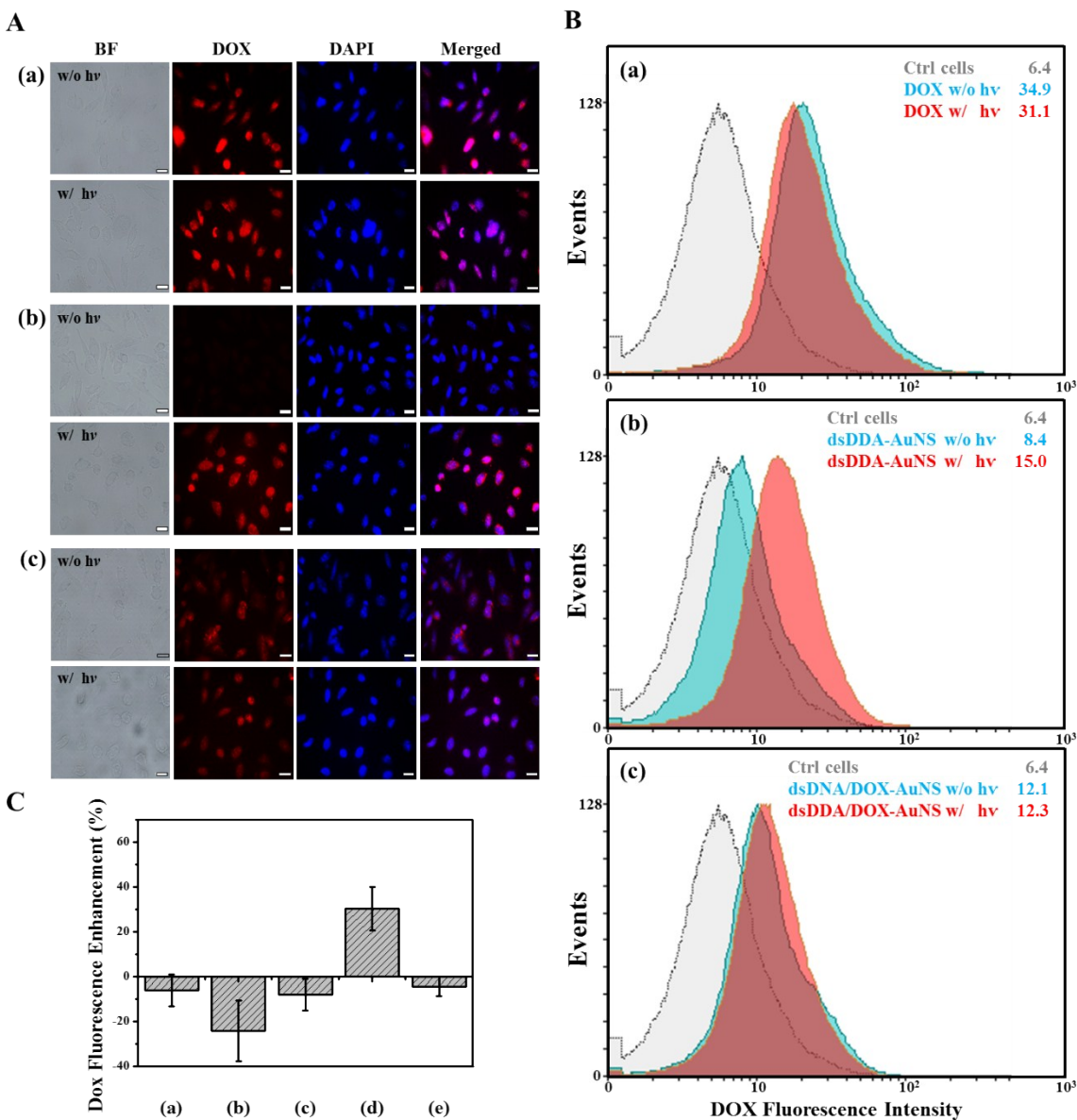


**Figure S16.** *In vitro* photo-triggered drug release of dsDDA-AuNS. (A) Microscopic images displaying the intracellular behavior of (a) free DOX, (b) dsDDA-AuNS (5  $\mu$ M DOX equivalents), and (c) dsDNA/DOX-AuNS inside TRAMP-C1 cells before and after NIR irradiation (808 nm, 1 W/cm<sup>2</sup>, 10 min). Cells were washed twice with washing buffer containing 1% BSA, stained with 4'-6-diamidino-2-phenylindole (DAPI), and fixed with 4% PFA for further analysis. Scale Bar: 20  $\mu$ m. (B) Flow cytometric histograms of cells treated with (a) free

DOX (4  $\mu$ M), (b) dsDDA-AuNS, and (c) dsDNA/DOX-AuNS, where populations are displayed as: control cells (gray), before (light blue) and after (red) laser irradiation. Cells were incubated with different samples in culture medium (10% FBS) for 12 h. Cells were then washed twice with washing buffer and exposed to NIR irradiation (808 nm, 1 W/cm<sup>2</sup>) for 10 min. (C) Increased percentage of intracellular DOX signals ( $\Delta F = (F_{(x)} - F_0)/F_0$ ) induced by NIR irradiation of (a) non-treated cells and cells treated with (b) free DOX, (c) dsDNA-AuNS, (d) dsDDA-AuNS, and (e) dsDNA/DOX-AuNS, respectively. All experiments were repeated at least three times.

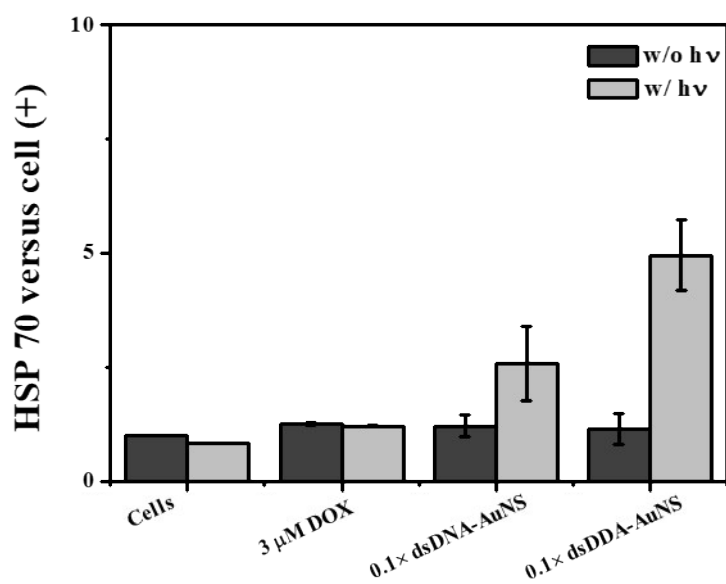


**Figure S17.** To confirm photothermally induced cellular deaths, the amounts of heat shock protein, HSP70, expressed at 37°C were determined from dsDNA-AuNS and dsDDA-AuNS internalized TRAMP-C1 cells followed by 10-min NIR light irradiation (1 W/cm<sup>2</sup>) with 3 h of recovery. The DOX and AuNS concentrations for 0.1× dsDDA-AuNS were 5.8 μM (12.5:1 DOX:DNA ratio) and 1.1 nM (0.1×), respectively.

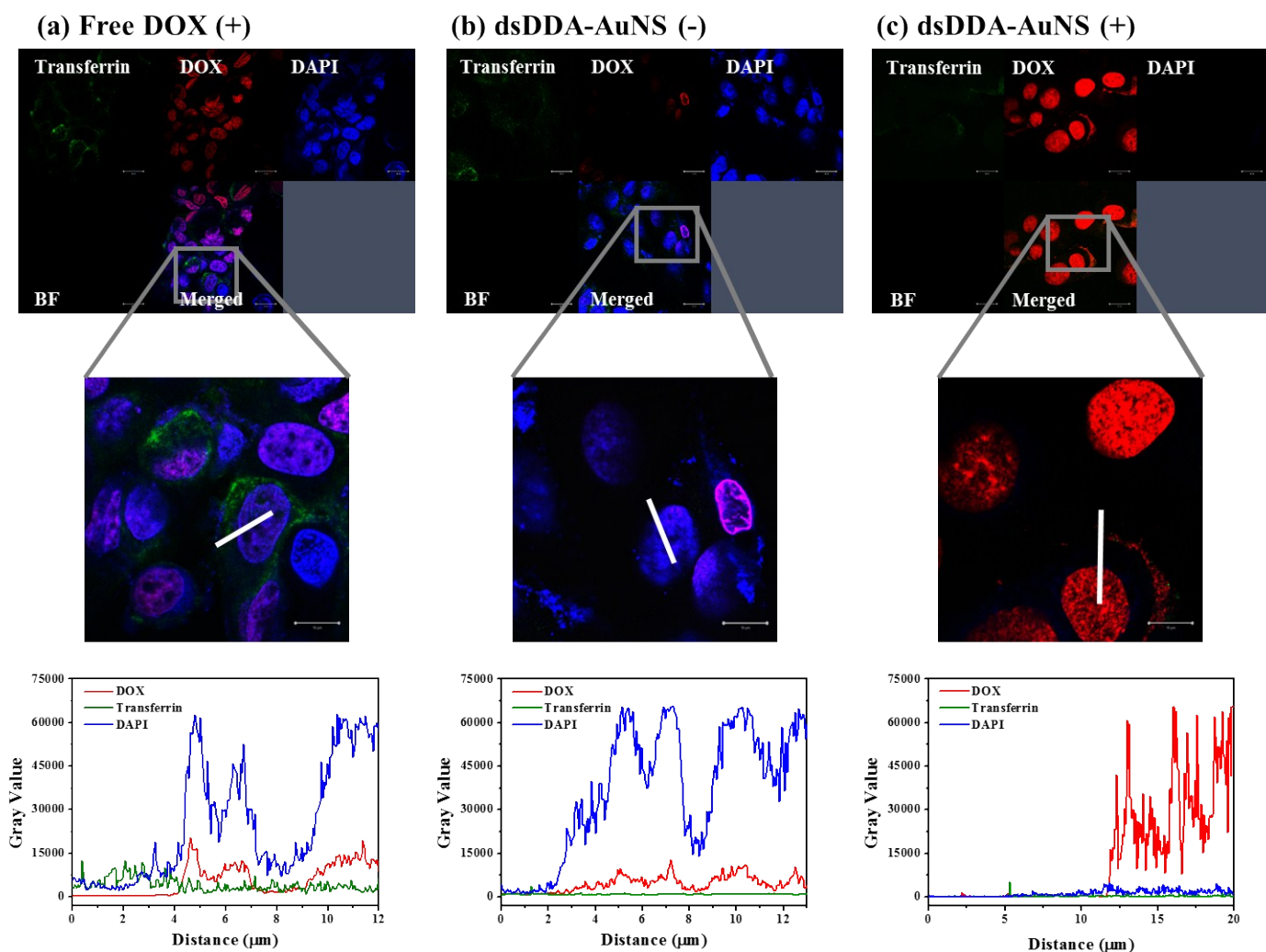


**Figure S18.** Intracellular delivery of DOX to the nucleus of MCF-7 cells with different treatments: (a) Dox with laser irradiation and dsDDA-AuNS (b) before and (c) after laser irradiation. Confocal fluorescence microscopic images demonstrating colocalization between AlexaFluor 633-transferrin (green), DOX (red), and DAPI (blue). Cells were exposed to different conjugates in culture medium (10% FBS) at 37°C for 12 h. Samples were removed and washed twice with washing buffer. After 808 nm laser irradiation (1 W/cm<sup>2</sup>, 10 min), cells were fixed

with 4% PFA for confocal analysis. The DOX and AuNS concentrations for all samples were kept constant at 11.7  $\mu\text{M}$  (12.5:1 DOX:DNA ratio) and 2.2 nM (0.2 $\times$ ), respectively. Scale Bars: 20  $\mu\text{m}$  and 10  $\mu\text{m}$  for split and cropped-magnified images, respectively.

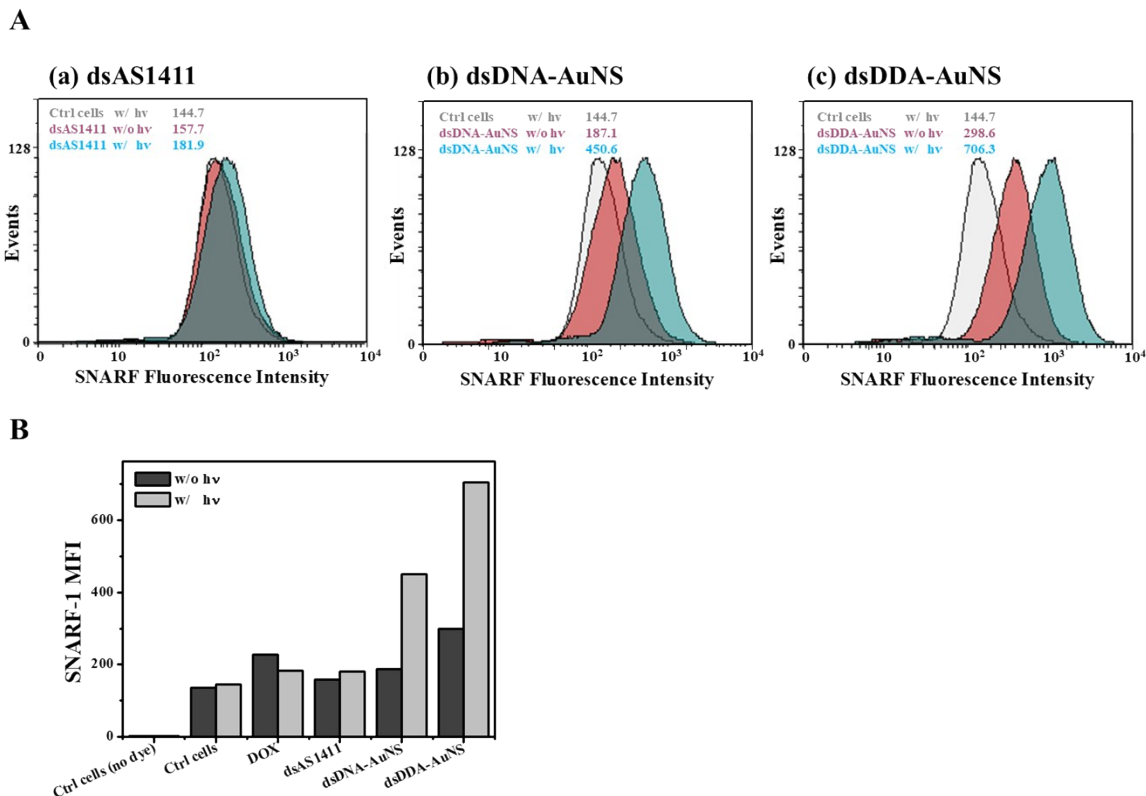
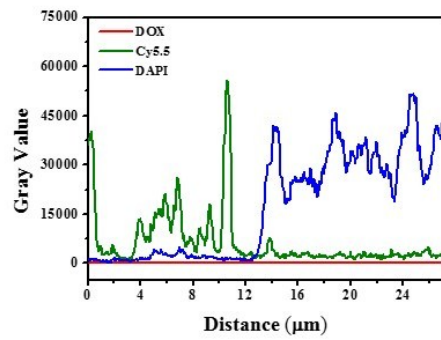
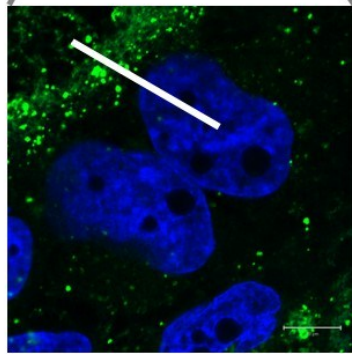
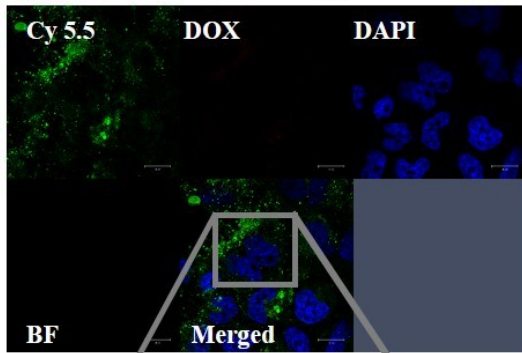


**Figure S19.** (A) Flow cytometric histograms of cytosol pH change in MCF-7/ADR cells treated with (a) dsAS1411, (b) dsDNA-AuNS, and (c) dsDDA-AuNS with (blue) or without (red) 10 min of irradiation (808 nm, 1 W/cm<sup>2</sup>), respectively. Non-treated cells are represented in gray. (B) Corresponding mean fluorescence intensity of MCF-7/ADR cells stained with SNARF-1. Cells were exposed to conjugates in culture medium (10% FBS) at 37°C for 12 h. After 808 nm laser irradiation (1 W/cm<sup>2</sup>, 10 min), cells were subsequently washed twice with washing buffer and stained with SNARF-1 according to the manufacturer's protocol. The fluorescence intensity increase was acquired via an APC channel (emission 640 nm). The DOX and AuNS concentrations for all samples were kept constant at 11.7 μM (12.5:1 DOX:DNA ratio) and 2.2 nM (0.2×), respectively.

(a) dsDDA-AuNS (-)



(b) dsDDA-AuNS (+)

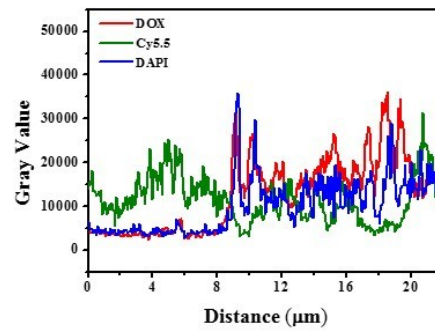
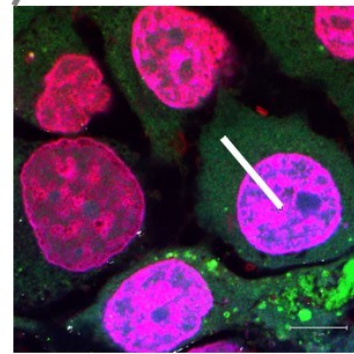
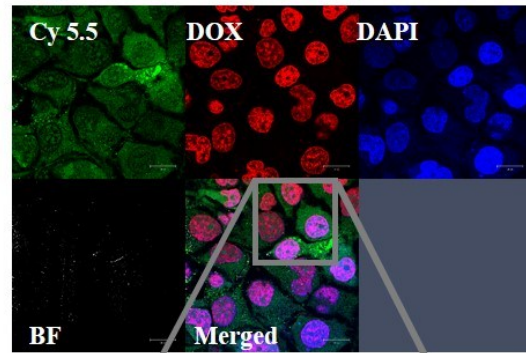
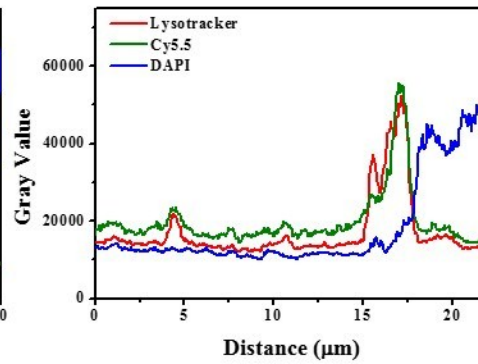
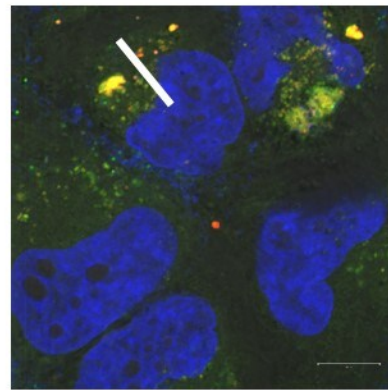
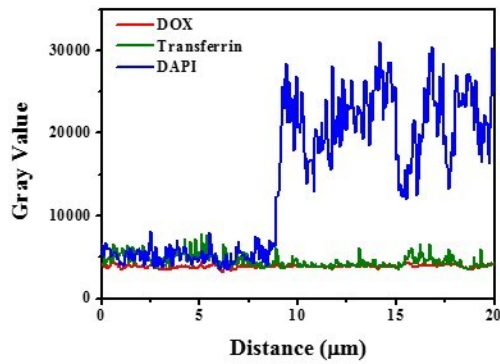
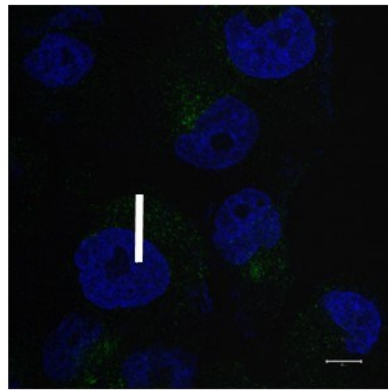


**Figure S20.** Intracellular trafficking of dsDDA-AuNS as well as the co-delivery of Cy5.5 labeled AS1411 and DOX to the nucleus. Confocal images of treated MCF-7/ADR cells was obtained (a) before and (b) after laser irradiation, with Cy5.5 labeled dsAS1411 (green), DOX (red), and DAPI (blue). Cells were exposed to conjugates in culture medium (10% FBS) at 37°C for 12 h and then washed twice with washing buffer and exposed to NIR irradiation (808 nm, 1 W/cm<sup>2</sup>) for 10 min. The DOX and AuNS concentrations for all samples were kept constant at 11.7 μM (12.5:1 DOX:DNA ratio) and 2.2 nM (0.2×), respectively. After irradiation, cells were subsequently fixed with 4% PFA for future analysis. Scale Bars: 20 μm and 10 μm for split and cropped-magnified images, respectively.

**(a) dsDDA<sub>MUC1</sub>-AuNS (-)**



**(b) dsDDA<sub>MUC1</sub>-AuNS (+)**

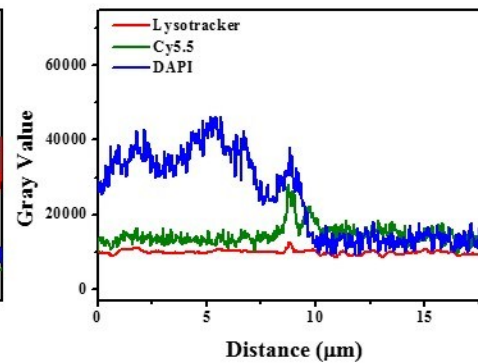
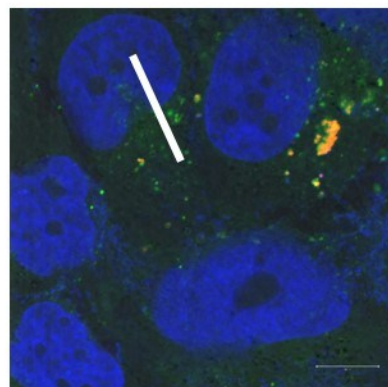
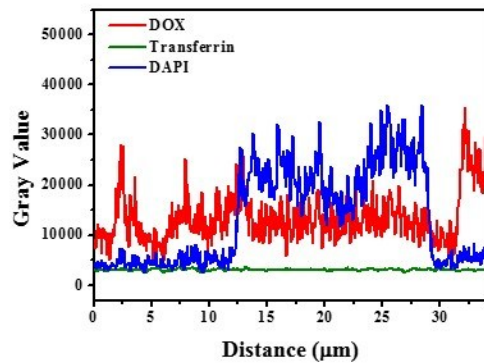
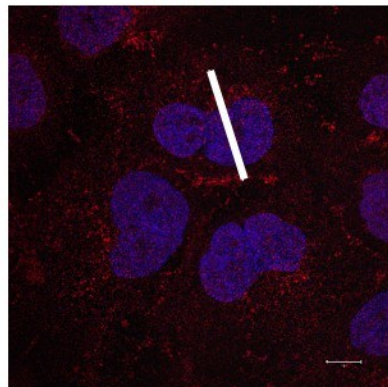
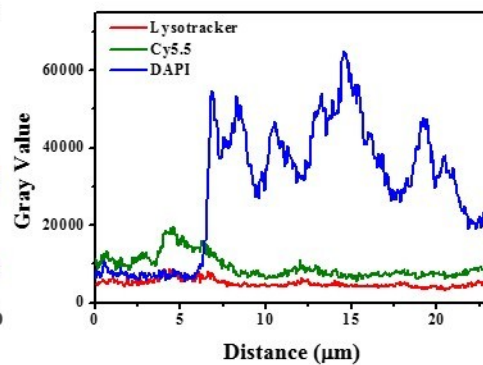
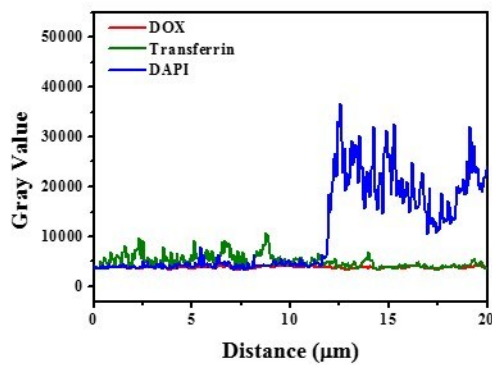
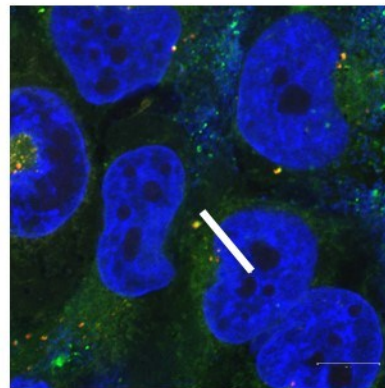
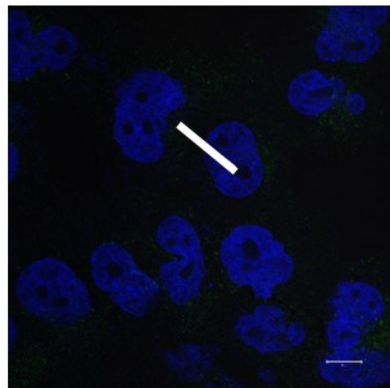


**Figure S21.** Confocal fluorescence microscopy colocalization between Left: unlabeled conjugate with AlexaFluor 633-transferrin (green), DOX (red), and DAPI (blue) and Right: labeled conjugate with Cy5.5-dsMUC1 (green), DOX (red), and DAPI (blue) staining of MCF-7/ADR cells incubated with dsDDA<sub>MUC1</sub>-AuNS (a) before and (b) after laser irradiation. The DOX and AuNS concentrations for all samples were kept constant at 5.8  $\mu$ M (3.12:1 DOX:DNA ratio) and 2.2 nM (0.2 $\times$ ), respectively. For both studies, MCF-7/ADR cells were exposed to different conjugates in culture medium (10% FBS) at 37°C for 12 h. Samples were removed and washed twice with washing buffer. After 808 nm laser irradiation (1 W/cm<sup>2</sup>, 10 min), cells were fixed with 4% PFA for confocal analysis. Scale Bar: 10  $\mu$ m and 15  $\mu$ m, left and right respectively.

**(a) dsDDA<sub>AS1411</sub>-AuNS (-)**



**(b) dsDDA<sub>AS1411</sub>-AuNS (+)**

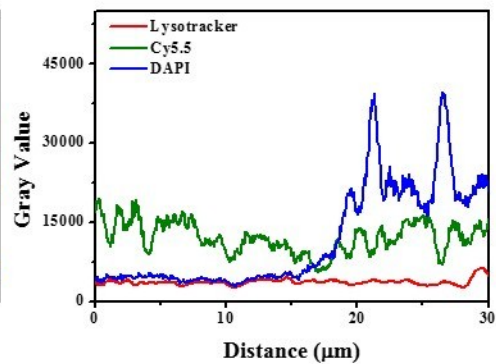
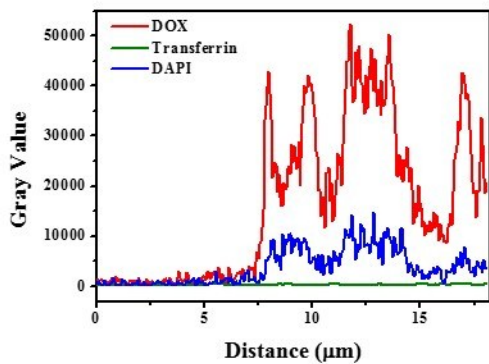
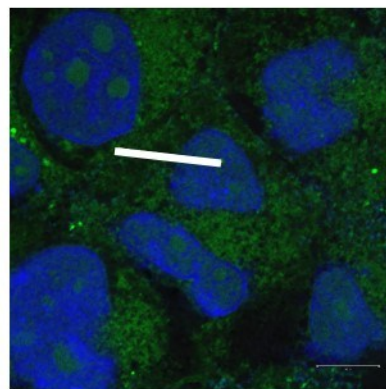
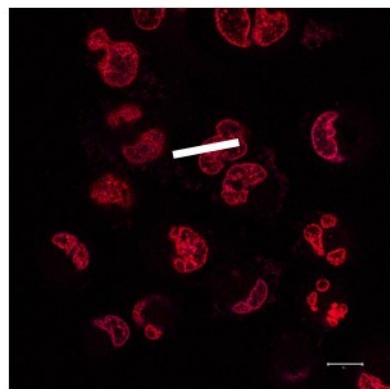


**Figure S22.** Confocal fluorescence microscopy colocalization between Left: unlabeled conjugate with AlexaFluor 633-transferrin (green), DOX (red), and DAPI (blue) and Right: labeled conjugate with Cy5.5-dsAS1411 (green), DOX (red), and DAPI (blue) staining of MCF-7/ADR cells incubated with dsDDA-AuNS (a) before and (b) after laser irradiation. The DOX and AuNS concentrations for all samples were kept constant at 5.8  $\mu\text{M}$  (3.12:1 DOX:DNA ratio) and 2.2 nM (0.2 $\times$ ), respectively. For both studies, MCF-7/ADR cells were exposed to conjugates in culture medium (10% FBS) at 37°C for 12 h. After 808 nm laser irradiation (1 W/cm<sup>2</sup>, 10 min), cells were subsequently and fixed with 4% PFA. Microscopic images are representative of three repeated experiments. Scale Bars: 10  $\mu\text{m}$  and 15  $\mu\text{m}$ , left and right respectively.

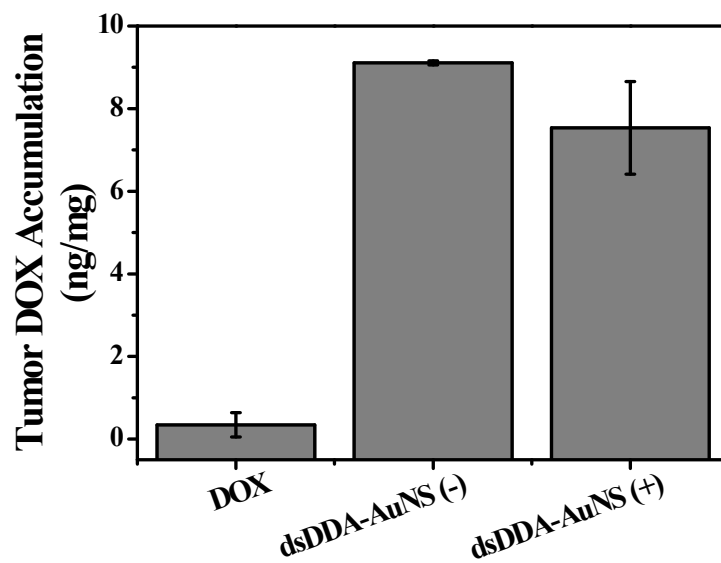


**Figure S23.** HPLC quantification of DOX accumulation in tumor tissue homogenates. After the single intravenous injection of DOX (0.125 mg per mouse) and dsDDA-AuNS (dose: 0.125 mg of Au; 2.3  $\mu$ g DOX per mouse), tumor-bearing mice were irradiated with 808 nm laser (0.9 mW/cm<sup>2</sup>, 3 min, 3 times at 5 min interval) on day 1 and day 2. Tumors were harvested and tissue homogenates were analyzed via HPLC.

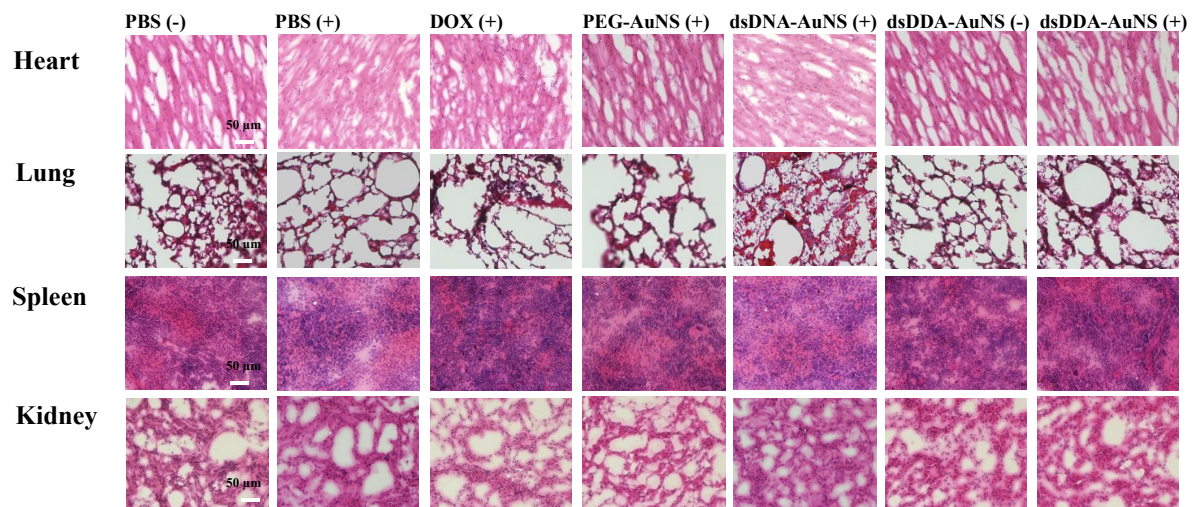


**Figure S24.** Histopathological analysis of major organs obtained from MCF-7/ADR tumor-bearing nude mice receiving different treatments. Treated mice were sacrificed and dissected to remove five organs at day 40 post-treatment. Scale bar = 50  $\mu$ m.

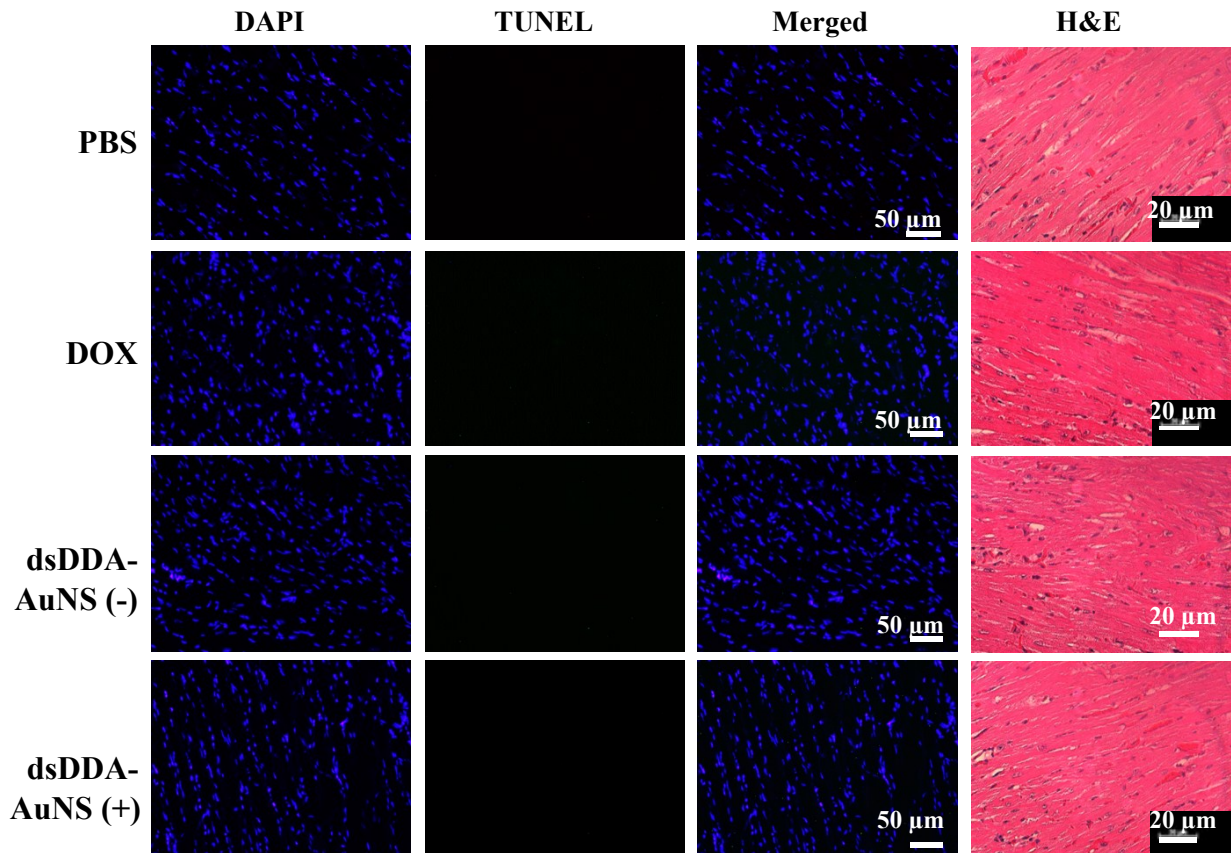


**Figure S25.** TUNEL fluorescence signal and H&E staining from heart tissues of tumor-bearing mice treated with PBS, DOX, dsDDA-AuNS (-) and dsDDA-AuNS (+), at day 40 post-treatment. Tissues were embedded in OCT and cryo-sectioned for microscopic images. Scale Bar: 50  $\mu\text{m}$  for fluorescence images and 20  $\mu\text{m}$  for H&E images, respectively.

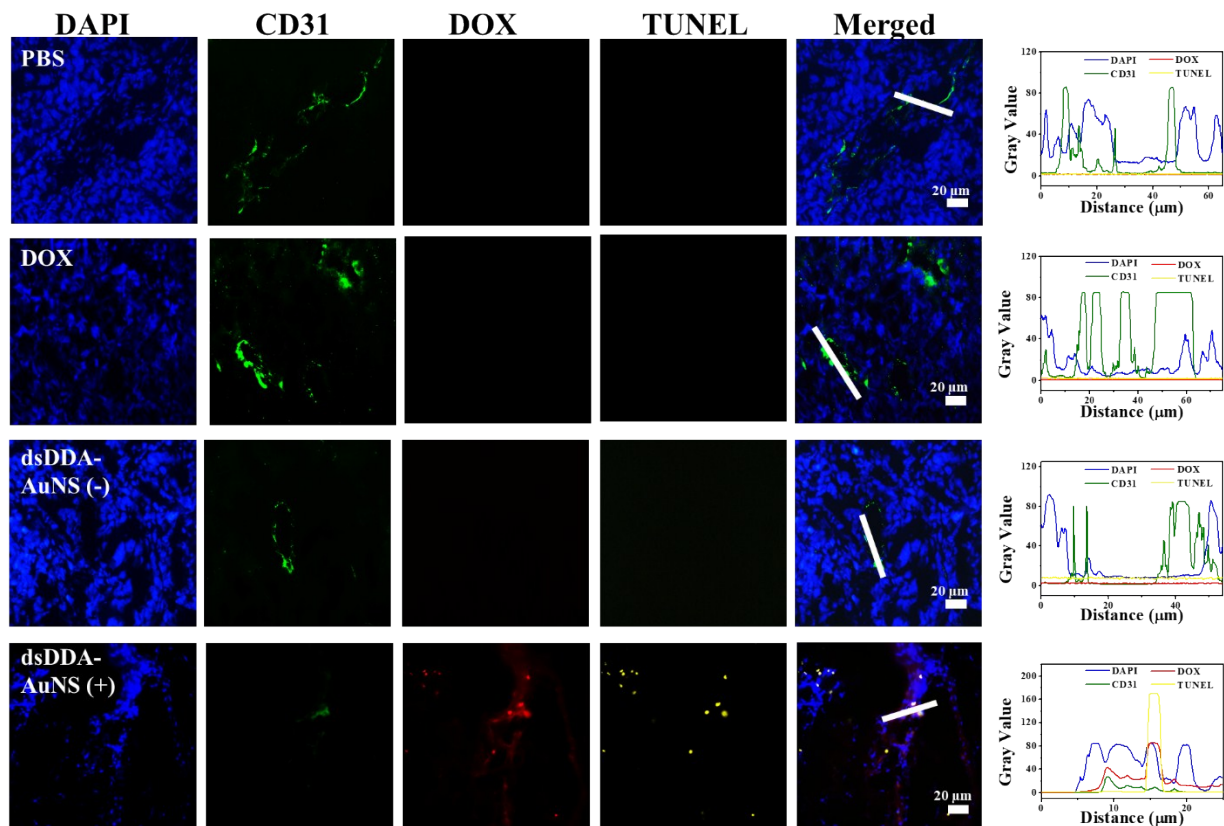


**Figure S26.** Tumor vascular distribution and fluorescence colocalization analysis of mice receiving different treatments. Immunohistochemical staining of xenograft MCF-7/ADR breast tumor tissues using CD31 and TUNEL assays was performed at 52 h post-treatment. All experimental conditions were identical to those in Figure 8. Scale bar: 20 μm.

## References

1. G. Frens, *Nat. Phys. Sci.*, 1973, **241**, 20.
2. S. J. Hurst, A. K. Lytton-Jean and C. A. Mirkin, *Anal. Chem.*, 2006, **78**, 8313-8318.
3. D. H. M. Dam, J. H. Lee, P. N. Sisco, D. T. Co, M. Zhang, M. R. Wasielewski and T. W. Odom, *ACS Nano*, 2012, **6**, 3318-3326.